Biochimica et Biophysica Acta, 1015 (1990) 156–171
Elsevier

BBABIO 43115

Investigations on the influence of headgroup substitution and isoprene side-chain length in the function of primary and secondary quinones of bacterial reaction centers

J.C. McComb, R.R. Stein and C.A. Wraight

Department of Physiology and Biophysics and Department of Plant Biology, University of Illinois, Urbana, IL (U.S.A.)

(Received 1 May 1989)
(Revised manuscript received 28 August 1989)

Key words: Reaction center; Bacterial photosynthesis; Quinone; Isoprene unit; (*Rb. sphaeroides*)

The contributions of headgroup and side-chain in the binding and function of the primary (Q_A) and secondary (Q_B) quinones of isolated reaction centers (RCs) from *Rhodobacter sphaeroides* were investigated. Various ubiquinones and structurally similar quinones were reconstituted into RCs depleted of one (1Q-RCs) or both (0Q-RCs) quinones. The influence of partition coefficients on the apparent binding affinities was minimized by expressing dissociation constants in terms of the mole fraction of quinone partitioned into the detergent. It was then apparent that the size of the isoprenyl side-chain was of little consequence in determining the binding affinity or the functional competence of either Q_A or Q_B, although an alkyl chain of equivalent size was a poor substitute. The degree of substitution of the headgroup, however, was a sensitive determinant of binding. For both quinone sites, the trisubstituted plastoquinones bound more weakly than the fully substituted ubiquinones. Similarly, for binding to the Q_A site, duroquinone (tetramethylbenzoquinone) bound much more strongly than trimethylbenzoquinone. The affinity of the Q_A site for ubiquinones was about 20-times stronger than the Q_B site, but the Q_B site is probably not more specific than the Q_A site. However, Q_B function depends on a suitable redox free-energy drop from Q_A as well as binding, and of all the quinones tested only the ubiquinones simultaneously supported full Q_A and Q_B activity. Even plastoquinone-A, which fills both roles in Photosystem II, was unable to do so in bacterial RCs, although it did bind. The unique ability of ubiquinones to both bind and provide the appropriate redox span is discussed. The temperature dependence of binding of the isoprenyl ubiquinones at the Q_A site changed markedly with chain length. For Q-10–Q-7, the binding enthalpy was positive and net binding was entirely driven by entropic factors. For the shorter-chain ubiquinones, Q-6–Q-1, both entropy and enthalpy of binding were favorable. This strong entropy-enthalpy compensation is suggested to arise from antagonistic interactions (anticooperativity) between headgroup and tail binding. For Q_B function by hydrophobic quinones, the temperature dependence of the micelle properties prevented easy access to thermodynamic parameters. However, for water-soluble Q-0, binding to the Q_B site was determined to be enthalpically driven. In the isoprenyl ubiquinone series, the electron transfer equilibrium for $Q_A^- Q_B \leftrightarrow Q_A Q_B^-$ declined gradually as the side-chain was shortened from 7 to 1 isoprene unit, in both 0Q and 1Q-RCs, implying that the in situ redox midpoint potential in the Q_B site decreased with decreasing side-chain length.

Introduction

Reaction centers from purple photosynthetic bacteria, and from Photosystem II of oxygenic organisms, provide reducing equivalents to a membrane pool of quinones which serves to reduce many secondary electron transport complexes [1]. The communication between the inherently one-electron events of the primary photochemistry and the two electron redox chemistry of quinones is achieved within the reaction center (RC) by means of a charge accumulating mechanism that includes a pair of specialized quinones, Q_A and Q_B [1,2]. From the recent X-ray structural analyses of the RCs from *Rhodopseudomonas viridis* [3,4] and *Rhodobacter sphaeroides* [5,6], it is known that the protein and cofactor arrangements display a strong two-fold rotational symmetry. Q_A and Q_B are bound, respectively, to the closely homologous M and L subunits, and are associated with an iron atom (high spin FeII). This structure constitutes the acceptor quinone complex which func-

Correspondence: C.A. Wraight, Department of Plant Biology, University of Illinois, 505, S. Goodwin Avenue, Urbana, IL 61801, U.S.A.

tions as a two-electron gate. In a series of flashes, the acceptor quinones are stepped through their functional redox states by electrons transferred from the excited singlet state of the primary donor, P, a dimer of bacteriochlorophyll [1]:

First Flash:

$$Q_AQ_B \xrightarrow{h\nu} Q_A^-Q_B \underset{(H^+)}{\overset{K_2}{\longleftrightarrow}} Q_AQ_B^-(H^+)$$

(stable semiquinone)

Second Flash:

$$Q_AQ_B^-(H^+) \xrightarrow{h\nu} Q_A^-Q_B^-(H^+)$$

$$\underset{(H^+)}{\overset{K_3}{\longleftrightarrow}} Q_AQ_BH_2 \overset{Q \quad QH_2}{\longleftrightarrow} Q_AQ_B$$

(The oxidized primary donor, P^+, is presumed to be rereduced after each flash by secondary donors, and turnover of P/P^+ is omitted in this scheme.)

This scheme clearly reveals the distinct properties of the primary and secondary quinones: Q_A acts exclusively as a one-electron component, whereas Q_B functions overall as a two-electron redox couple, with a stable one-electron intermediate state, the semiquinone. A further distinction between the two is that Q_A is tightly bound and does not normally exchange, while rapid binding and unbinding of quinone and quinol forms is an intrinsic part of the normal functioning of Q_B [2]. The redox properties that underlie these very different behaviors can be generally ascribed to the influence of the protein environment on the quinones, in their respective binding sites. This is most evident in those cases where Q_A and Q_B roles are filled by the same chemical species, such as ubiquinone-10 (Q-10), which is the only electron-transport-active quinone in *Rb. sphaeroides.*

The interactions that give rise to the specific properties of Q_A and Q_B are, of course, mutual between protein and quinone, and an understanding of the two-electron gate requires examination of the structural and electronic attributes of both. The recent advances in our knowledge of the protein have tended to overshadow the importance of the quinones themselves. However, major steps have been taken towards establishing the ground rules of quinone electrochemistry [7,8] and their contributions towards the specificity of binding and redox function in the Q_A site of RCs from *Rb. sphaeroides* [9,10]. In this work we have examined the ubiquinone isoprene homologues ('prenylogues', Q-1 through Q-10), and some closely related analogue structures, to address the question of specificity of quinone function in both the Q_A and Q_B sites of RCs from *Rb. sphaeroides.* Our findings indicate that the specificity of either site is not great but, of all the quinones tested, only the ubiquinones (2,3-dimethoxy-5-methylbenzoquinones) were able to simultaneously satisfy both roles. This attribute is discussed in terms of site-selective tuning of the ubiquinone redox midpoint potentials, through the disposition of the methoxy groups [7,11].

Materials and Methods

Reaction centers were isolated from chromatophore membranes of *Rb. sphaeroides*, strain R-26, by fractionation of the membranes with 0.45% lauryldimethylamine *N*-oxide (LDAO or Ammonyx LO; Onyx Corporation, NJ) in 100 mM NaCl/10 mM Tris (pH 8.0), essentially as described elsewhere [12]. The RCs were purified by column chromatography on DEAE-Sephacel (Pharmacia) and eluted in 160 mM NaCl/0.1% LDAO/10 mM Tris (pH 8.0).

Reaction center quinones (Q_A and/or Q_B) were extracted essentially as described by Okamura et al. [13], by washing with selected levels of *o*-phenanthroline and LDAO, on a DEAE column. RCs were prepared containing 0.8–1.05 Q-10/RC ('1Q-RCs') or 0.0–0.15 Q-10/RC ('0Q-RC's'). The extractant solution was kept anaerobic (N_2 purge) and dithiothreitol (2 mg/l) was added as a protein stabilizing agent and mild reductant. After washing to remove the *o*-phenanthroline and excess LDAO, the extracted RCs were eluted with 0.25 M NaCl/0.1% LDAO/10 mM Tris (pH 8.0). RCs were concentrated by ultrafiltration (Amicon XM-100 membrane) and repeatedly diluted with aliquots of 10 mM Tris, 0.1% LDAO (pH 8.0), to remove the salt.

Ubiquinones-10, -9 and -7 were obtained from Sigma (St. Louis, MO). Synthetic ubiquinones-6 through 1 were a generous gift of the Esai Corporation, Japan. 2,3-Dimethoxy-5-methylbenzoquinone (Q-0) and 2,3-dimethoxy-5,6-dimethylbenzoquinone (methyl-Q-0) were obtained from Spectrum Chemical Mfg. Corp., Gardena, CA. 2,3-Dimethoxy-5-methyl-6-decylbenzoquinone (decy-Q-0) was a generous gift from Dr. C.A. Yu (Stillwater, OK). All ubiquinones from these sources were used without further purification. Ubiquinone-8 (Q-8) and menaquinone-8 (MK-8) were isolated from *Escherichia coli*, and purified by column chromatography [14]. Plastoquinones A, B and C were isolated from spinach chloroplasts as described by Barr and Crane [15]. Phylloquinone (vitamin K-1, 2-methyl-3-phytyl-1,4-naphthoquinone, phytyl-MK-0) and D-α-tocopherolquinone were obtained from Calbiochem, La Jolla, CA. All other commercially available quinones were further purified by recrystallization from ethanol and/or by sublimation in vacuo.

All ubiquinone stocks were assayed, after dilution into ethanol, from their ultraviolet difference spectrum: oxidized-minus-reduced (borohydride) $\Delta\varepsilon_{275} = 12.2$ $mM^{-1} \cdot cm^{-1}$ [16]. Menaquinone-8 and phylloquinone

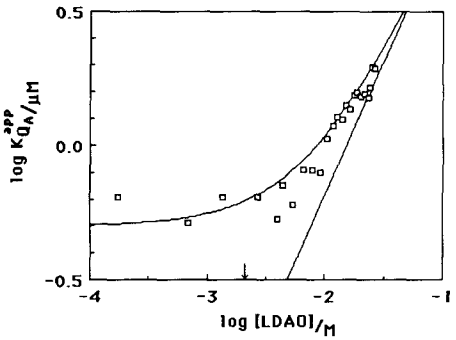

Fig. 1. The apparent binding affinity for duroquinone at the Q_A site, as a function of detergent (LDAO) concentration. Conditions: 0.5 μM RCs, 10 mM Tris (pH 8.0). The critical micelle concentration for LDAO (CMC = 2.1 mM) is indicated by the arrow on the abscissa. The curve drawn indicates the expected behaviour for an aqueous dissociation constant (at zero detergent) $K_{Q_A}^{aq} = 0.5$ μM, and partition of duroquinone into the detergent micelles according to log $P = 2.7$. The line represents the asymptote at high detergent concentration.

were assayed similarly, using $\Delta\varepsilon_{265-289} = 14.7$ $mM^{-1} \cdot cm^{-1}$ [17]. The RC concentration of samples was routinely determined by flash induced absorption changes in the presence of an excess of Q-10 ($\Delta\varepsilon_{602} = 26$ $mM^{-1} \cdot cm^{-1}$).

Buffers used over various ranges of pH were as follows: pH 6.5–8.0, Hepes; pH 8.0–9.0, Tris; pH 9.0–10.2, glycine; and above pH 10.2, 3-(cyclohexylamino)propanesulfonic acid (Caps) (all from Sigma).

Optical measurement were performed on an unchapped, dual-beam spectrophotometer of local design. Flash saturation was routinely checked in a series of closely spaced flashes and was always above 95%. An LSI-11/73 minicomputer (Digital Equipment Corp., Cambridge, MA) was used to control data acquisition and to reduce data. Data was gathered via a 135 kHz, 12 bit (0.002%) resolution, 8 channel, differential input, A/D converter (DT2782, Data Translation, MA). The computer was used to signal average, perform linear least-squares analysis, and to run a modified Marquardt non-linear least-squares regression on multicomponent exponential decay curves [18].

Determination of Q_A binding and function

Quinone binding to the Q_A and Q_B sites of RCs was determined by functional assays. Q_A was assayed by the ability to generate a long-lived (> 10 μs) charge separation state, $P^+Q_A^-$. The quantum yield (ϕ) for charge separation in native RCs is very close to 1.0 [19], and previous work has shown that substitution of Q_A by a wide variety of quinones does not significantly alter this value, providing the redox midpoint potential of the quinone is not very low [9,10,22]. In fact the forward electron transfer leading to the charge separation is sufficiently fast, compared to any unproductive back-reactions from P^+I^-, that considerable changes in the forward rate can be accommodated without measurably affecting the quantum yield of $P^+Q_A^-$ formation. Using the facilities of the Laser Laboratory (Department of Chemistry, University of Illinois), we have measured directly the electron transfer from P^+I^- to $P^+Q_A^-$ in RCs reconstituted with duroquinone as Q_A and find that the forward electron transfer rate for duroquinone is slower than for Q-10 ($\tau_f = 565$ ps vs. 215 ps) (not shown). However, the unproductive back-reaction, apparent in fully extracted, unreconstituted RCs, is much slower still ($\tau_b = 12$ nm; see Ref. 20 for review of primary kinetics), giving an expected quantum yield of 0.96 for $P^+Q_A^-$ formation with duroquinone as Q_A ($\phi = \tau_b/[\tau_f + \tau_b]$). This is in agreement with the assessment of Pocinki and Blankenship [21], who found the quantum yield for duroquinone-reconstituted RCs to be indistinguishable from that of native RCs. For all of the quinones used in this work, which does not include any low-potential varieties, we have taken $\phi = 1.0$ and have used the amplitude of the flash-induced P^+ signal as a measure of quinone binding in the Q_A site *.

For the more hydrophobic ubiquinones, stock solutions were prepared by suspension in concentrated detergent (30%, v/v) by sonication followed by repeated freezing and thawing until a translucent mixture was obtained. Less elaborate procedures, or use of ethanolic stocks, resulted in substantial losses of effective concentration for all the long-chain ubiquinones (Q-10–Q-7). We presume that this is due to the persistence of microcrystalline or colloidal forms of the quinones. Samples containing the long-chain prenylogues were prepared by progressive dilution with buffer, keeping the detergent at or above the final concentration to be used, and then adding RCs from another concentrated stock solution. Smaller benzoquinone derivatives, including Q-1 and Q-2, were routinely added from ethanolic stocks.

Because of the strong affinity of the ubiquinones for the Q_A site, the Q_A titrations were very sensitive to errors in determining the concentration of free quinone, i.e., by subtracting out the amount bound from the total added. To minimize this source of error, and at the same time to enhance the quantitative dissolution of the long-chain prenylogues in the sample, we determined

* Our routine experimental set up utilizes a xenon flash lamp rather than a laser. This adds the potential difficulty that for quinones of low ϕ the unproductive decay of P^+I^- to the ground state is fast compared to the flash duration (half width approx. 10 μs), allowing the possibility of reexcitation during the flash. The result is 'pumping' into the $P^+Q_A^-$ state with high apparent yield. This effect is partially mitigated by the fact that decay of a significant portion of the intermediate state, at ambient temperatures, involves formation of the molecular triplet (^3P), which then decays with a lifetime of several microseconds under anaerobic conditions, thereby preventing pumping. In any case, this problem does not arise if ϕ is high.

the overall Q_A binding affinity (K_{Q_A}) in the presence of relatively high detergent levels – 0.3% LDAO. The very hydrophobic nature of most of the quinones used means that they are almost exclusively partitioned into the detergent micelle phase, and the effective concentration is best described by the mole fraction in the detergent, $X_q^{det} = N_q/(N_q + N_{det})$, where N_q and N_{det} are the total number of moles of quinone and detergent, respectively. One might suppose that this should be expressed in terms of micelle detergent, i.e., $N_q/(N_q + N_{det} - N_{cmc})$, where N_{cmc} in the number of moles of monomeric detergent corresponding to the critical micelle concentration (cmc). However, in the presence of a membrane protein like the RC, protein-detergent mixed micelles are likely to form at all concentrations.

We have established in this work (see below) that all hydrophobic quinones, including the isoprenyl ubiquinones (but not Q-0 and methyl-Q-0), function in the manner expected for complete partition into the detergent phase. Diner showed that the solubility of Q-1 in water is about 1 mM, but that it can dissolve to at least 50 mM in 3.0% (136 mM) LDAO [23]. From this, one can calculate a minimum partition coefficient for Q-1 between the detergent micelle phase and water: log $P = 3.2$. This value is somewhat higher than estimates of the partition coefficient in cyclohexane (log $P = 2.7$) taken from the work of Dutton and co-workers, who have correlated mobility in reverse-phase HPLC with partition coefficients determined by the shake-flask method [24,25]. Similarly, in crude estimates of the partition of Q-0 into LDAO, we have found values of log P 0.4–0.7 units higher than literature values for partition into cyclohexane. These values of log P for ubiquinone derivatives are more in line with literature determinations in octanol, which are about 0.4 units higher than cyclohexane values for a wide range of quinones [24,25]. Knowledge of the partition of quinone into the detergent phase is essential for understanding the behaviour of quinones of intermediate hydrophobicity, which partition incompletely into the micelles. For this purpose we have taken log P for ubiquinone derivatives (Q-0, methyl-Q-0 and Q-1) either from octanol data or by adding 0.4 to the more numerous cyclohexane data.

Even small molecules such as duroquinone (2,3,5,6-tetramethylbenzoquinone) can be sufficiently hydrophobic as to partition readily into the detergent phase. This is as expected from the partition coefficient of duroquinone (log $P = 2.6$ in octanol [24,25]). Fig. 1 shows the effective dissociation constant for duroquinone, reconstituting Q_A activity, as a function of the concentration of LDAO as detergent. At low levels the quinone affinity is constant and reflects the binding equilibrium for quinone from the aqueous bulk phase, in which duroquinone is barely soluble. The values we obtain fall between those reported earlier in low detergent, by Gunner et al. ($K_{Q_A} = 0.1$–0.3 μM below the CMC of LDAO, (Ref. 25, and M. Gunner, personal communication), and that in high detergent, by Pocinki and Blankenship ($K_{Q_A} = 18$ μM in 1.0% LDAO [21]), and can be taken to reconcile these discrepant values. However, in contrast to our findings, the latter workers concluded that the binding affinity of duroquinone was not sensitive to detergent concentration. Fig. 1 clearly shows that at high detergent concentrations, the apparent affinity for duroquinone decreases as it partitions into the detergent micelles, with log $P = 2.7$. At high detergent levels the apparent affinity tends towards a linear function of the detergent concentration, as expected from this description. Almost identical results were obtained in Triton X-100 (not shown).

Determination of Q_B binding and function

Q_B binding and function were assayed by a variety of techniques, with varied applicability.

Assays of charge recombination

With only Q_A active, the state $P^+Q_A^-$ recombines in a characteristic time of 70–100 ms, with ubiquinone as Q_A. If electron transfer to Q_B occurs, the reappearance of P occurs with a half-time of about 1.0 s. This retardation arises because the back-reaction occurs only from the $P^+Q_A^-$ state and electron transfer to Q_B ($P^+Q_A^-Q_B \leftrightarrow P^+Q_AQ_B^-$) diminishes the time averaged population of Q_A^- [27,28]. Thus, the kinetics of P^+ rereduction are modified according to the electron transfer equilibrium, K_2, which is rapid compared to the recombination of $P^+Q_A^-$. The activity of Q_B is also determined by a binding equilibrium with free quinone that is established on a timescale that can be relevant to the recombination kinetics, and the binding must be included explicitly [29,30]:

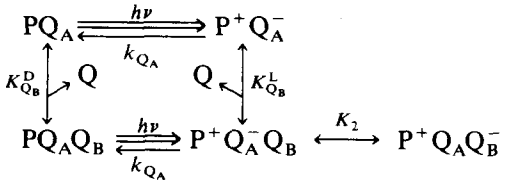

If the binding equilibrium is established rapidly compared to the recombination process from $P^+Q_A^-$, the overall recombination from $P^+Q_B^-$ occurs with an apparent rate constant, k_{Q_B}, given by [29]:

$$k_{Q_B} = k_{Q_A}/[1 + K_2^{app}] \tag{1A}$$

where

$$K_2^{app} = K_2 \frac{[Q]/K_{Q_B}^L}{1 + [Q]/K_{Q_B}^L} \tag{1B}$$

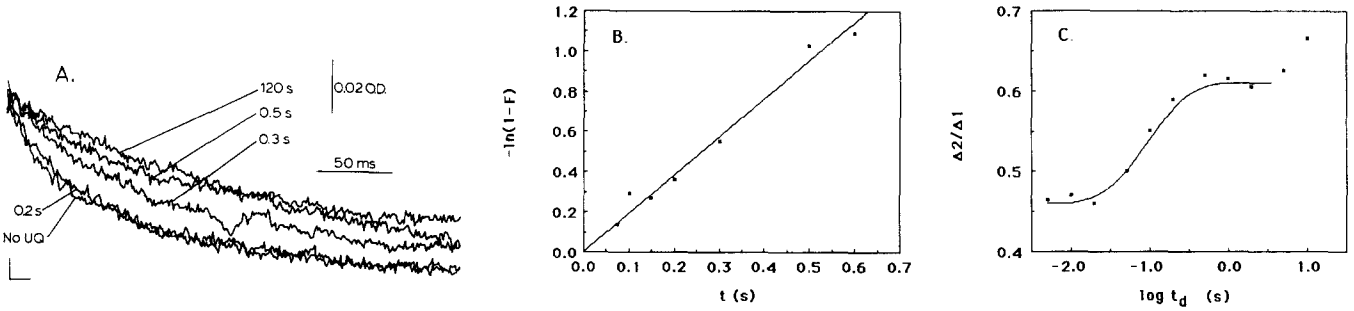

Fig. 2. Time dependence of Q_B activity in detergent suspensions. (A) Kinetics of charge recombination at various times after mixing RCs (approx. 1.3 Q/RC) with excess Q-10. Equal volumes of RCs and Q-10 in 10 mM Tris (pH 8.0)/0.1% LDAO, were rapidly mixed to yield final concentrations of 5 μM RCs and 33 μM Q-10. A single flash was given at various times after mixing, and the recombination kinetics recorded at 430 nm. The beginning of the trace was synchronized to the flash. (B) Plot of the data from part A. To account for the Q_B activity at $t = 0$, due to residual quinone in the unmixed RCs, the data are expressed as:

$$F = \frac{[\Delta F(t) - \Delta F(t=0)]}{[\Delta F(t=\infty) - \Delta F(t=0)]}$$

where ΔF is the amplitude of the fast phase of the recombination kinetics, characteristic of RCs lacking Q_B. (C) Evolution of Q_B activity in Triton X-100, using a double flash assay of cytochrome *c* turnover. The relative amplitude of cytochrome *c* oxidation on the second of two flashes ($\Delta 2/\Delta 1$) is plotted against the dark time between flashes. Conditions: 0.8 μM RCs, 1.6 μM Q-10, 45 μM cytochrome *c*, 0.03% Triton X-100, 10 mM Tris (pH 8.0 at 23° C). The line is drawn for a half time of 90 ms for the increase in second flash activity

The dissociation constant, $K^L_{Q_B}$, describes the binding of quinone with RCs in the state $P^+Q_A^-$, i.e., the post-flash equilibrium. The characteristic feature of this situation is that the rereduction of P^+ should be monophasic and exhibit a quinone concentration-dependent rate constant. Quinone titration of the rate of the recombination reaction will yield $K^L_{Q_B}$ and K_2 directly, e.g., from the *x* and *y* intercepts when plotted as $1/(k_{Q_A}/k_{Q_B} - 1)$ vs. 1/[Q]. This approach works well for the most water-soluble quinones, 2,3-dimethoxy-5-methylbenzoquinone (Q-0) and 2,3-dimethoxy-5,6-dimethylbenzoquinone (methyl-Q-0), as demonstrated previously for Q-0 [29].

On the other hand, if the binding equilibrium is slow compared to the net $P^+Q_B^-$ recombination process, a mixed population of Q_B-containing and Q_B-lacking RCs will give rise to biphasic kinetics of P^+ rereduction. The two phases will exhibit quinone concentration-independent rate constants equal to k_{Q_A} and $k^o_{Q_B}$, the recombination rate when quinone is fully bound as Q_B, viz., Eqn. 1A when the binding equilibrium is saturated ($k^o_{Q_B} = k_{Q_A}/[1 + K_2]$). The amplitudes of the two phases were determined by the degree of binding of quinone with RCs in the state PQ_A, according to $K^D_{Q_B}$, i.e., the dark (or pre-flash) equilibrium. Thus, $K^D_{Q_B}$ can be obtained from a titration of the amplitude of the slow phase, ΔS, vs. [Q] [18,29].

In the general case, when the quinone binding equilibrium is on the same time-scale as the recombination events, the kinetics will also be biphasic, but with apparent rate constants that are quinone concentration-dependent and do not correspond exactly to k_{Q_A} and $k^o_{Q_B}$. The amplitudes of the phases will also not truly reflect the preflash quinone binding equilibrium. Titration of the recombination kinetics with quinone is then only a rough guide to the quinone binding properties, although quantitative data can be extracted by simulation of the complex, mixed order kinetics [18,31].

The effect of Q_B on the back reaction also provides an experimental assay of the electron transfer between Q_A and Q_B [27,28,32]. Thus, the recombination rate when the Q_B site is saturated reflects the intrinsic electron transfer equilibrium. By rearrangement of Eqn. 1A we obtain:

$$K_2 = (k_{Q_A}/k^o_{Q_B}) - 1 \qquad (2)$$

For different degrees of mobility of the quinone, however, knowing whether a measured k_{Q_B} is really at the limit ($k^o_{Q_B}$), or not, can be problematical, and this is returned to later.

Direct assay of Q_A^- to Q_B electron transfer

In an earlier study, we showed that the amplitude of the slow phase of P^+ rereduction, in isolated RCs with Q-10 as Q_B, corresponded well with the amplitude of a submillisecond absorbance transient at about 400 nm (typically 397 nm) that indicates the electron transfer from Q_A^- to Q_B [29]. This correspondence shows that the slow recombination phase reflects Q_B that is bound or rapidly available at the time of the flash, and that equilibration of quinone binding involving transfer between micelles is slow for isolated RCs suspended in detergent. This was generally true for RCs reconstituted with long chain prenyl ubiquinones in LDAO suspensions, and was also true for RCs suspended in Triton provided the temperature was not much above 21° C. At

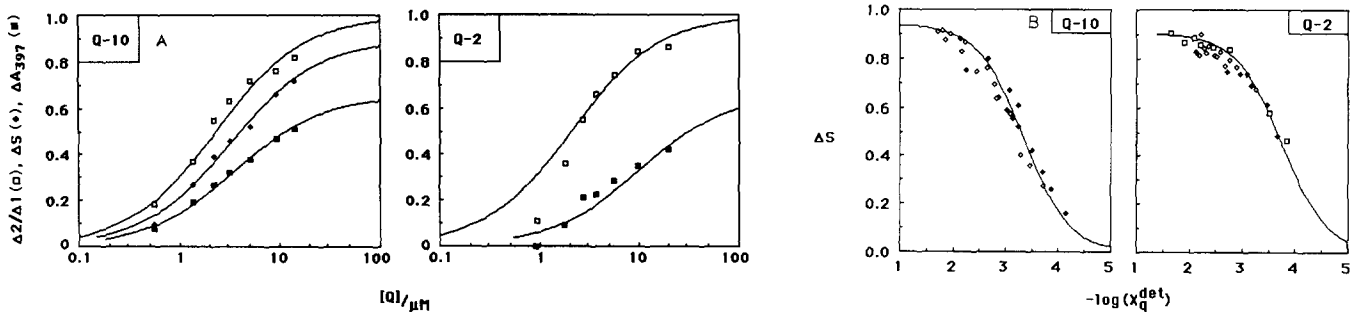

Fig. 3. Dependence of Q_B activity on quinone and detergent concentration. (A) Comparison of different assays: (□) cytochrome *c* double flash assay ($\Delta 2/\Delta 1$), $t_d = 1$ s; (◆) relative amplitude of the slow component of the recombination kinetics (ΔS); (■) amplitude of the millisecond transient at 397 nm (ΔA_{397}), indicative of electron transfer from Q_A^- to Q_B, relative to the instantaneous change ($P^+Q_A^-$). Conditions: 0.5 μM RCs, 10 mM Tris (pH 8.0) and 0.06% Triton X-100, 23° C; (□) plus 24 μM cytochrome *c*. Lines are drawn according to binding isotherms with maximum values of: 1.0 (□), 0.9 (◆) and 0.66 (■). (B) Comparison of detergents and detergent concentration; Q_B assayed by the slow component of recombination (ΔS). Left: Q-10 in Triton X-100 (◇) and LDAO (◆); detergent concentration was varied at two, constant quinone concentrations (3 and 13 μM). Approx. 1 μM RCs, 10 mM Tris (pH 8.2, 17° C). Right: Q-2 in LDAO; quinone concentration was varied at three different detergent levels (□, 0.025%; ◇, 0.1%; ◆, 0.3%). Approx. 0.5 μM RCs, 10 mM Tris (pH 8.0, 23° C). Lines are drawn for binding isotherms with: left, $\Delta S_{max} = 0.94$, $\log X_{Q_A}^{det} = 3.35$ (the Triton and LDAO data are best fit separately with $\log X_{Q_A}^{det} = 3.25$ and 3.45, respectively); right, $\Delta S_{max} = 0.9$, $\log X_{Q_A}^{det} = 3.7$.

higher temperatures, in Triton, the two measures (ΔS and ΔA_{397}) showed some divergence, indicating that the rate of quinone binding and exchange became significant on the back reaction timescale. It was suggested that the slowness of the quinone binding equilibrium was a reflection of the rate limiting transfer of quinone from a quinone-detergent micelle to a reaction center-detergent micelle. This was studied by measuring the rate of appearance of a slow recombination phase after rapid mixing of excess quinone (Q-10) with RCs lacking Q_B (Fig. 2A,B). The recombination kinetics were recorded following a flash given at various times after mixing in an Aminco-Morrow W-2 Stopped Flow Accessory attached to the kinetic spectrophotometer. In LDAO, the ability to exhibit a slow phase appeared in 0.3–0.7 s, whereas in Triton the slow-phase behavior appeared in less than 100 ms [18].

Since the submillisecond electron transfer from Q_A^- to Q_B is much faster than any intermicelle quinone transfer, the amplitude of the transient at 397 nm (ΔA_{397}) is a good measure of the pre-flash quinone binding equilibrium, $K_{Q_B}^D$, except when the quinone is rapidly mobile in the aqueous phase. This method is especially useful for fairly hydrophobic quinones such as Q-1, Q-2 and decyl-Q-0 (2,3-dimethoxy-5-methyl-6-decylbenzoquinone). For these, the mobility is significant compared to the back reaction, so that ΔS is not an accurate reflection of the pre-flash binding equilibrium, but it is not so fast that the slow recombination rate, k_{Q_B}, is a good measure of the post-flash equilibrium.

For quinones that are very rapidly mobile through the water phase, e.g., Q-0 and methyl-Q-0, the amplitude of Q_A^- to Q_B electron transfer (ΔA_{397}) includes a significant contribution from quinone that is bound as Q_B after the flash. Even if the Q_B binding affinity is the same for PQ_A and $P^+Q_A^-$ ($K_{Q_B}^D = K_{Q_B}^L$), the effective binding affinity after the flash will be greater than before, because the electron transfer from Q_A^- to Q_B will pull the equilibrium over [18,29]:

$$K_{Q_B}^{app} = K_{Q_B}^L/[1 + K_2] \quad (3)$$

In such cases, K_2 and K_{Q_B} must be obtained from titrations of Q_B activity, as described above, using Eqns. 1.

Assay of reaction center turnover

Another assay of quinone binding to the Q_B site is the ability of the RC to oxidize exogenous donors in a series of flashes (turnover). Rereduction of P^+ following a flash traps the RC in the states PQ_A^- or $PQ_AQ_B^-$; only the latter is capable of further turnovers and, thus, the second flash activity is an assay of Q_B function. Since the states PQ_A^- and $PQ_AQ_B^-$ are long-lived, the second flash can be delivered at quite long times after the first, allowing time for even quite slow quinone binding events to come to equilibrium. By varying the time between flashes (t_d) one can assay the dark (at short t_d) or light (at long t_d) binding equilibria, or the evolution from one to the other, i.e., the rate of arrival of quinones after the flash. This method is illustrated in Fig. 2C, which shows the evolution of Q_B activity for Q-10 in RCs in Triton. The significant mobility of Q-10 in this detergent is apparent in the increase in turnover observed for dark times in the range of 30–200 ms ($t_{1/2} = 90$ ms). At longer times, a second phase of enhancement is seen, corresponding to net reoxidation of Q_A^- formed on the first flash.

Applicability of Q_B assay methods

The various assays for Q_B activity were tested with Q-1, Q-2, Q-6 and Q-10 in both LDAO and Triton, and

the apparent dissociation constants, when distinguishable, were always in the order expected: $K_{Q_B}^{app}(\Delta A_{397}) \geq K_{Q_B}^{app}(\Delta S) \geq K_{Q_B}^{app}(\Delta 2/\Delta 1)$ (Fig. 3A). It should be noted, however, that for mobile species ΔS is not a suitable observable, as the kinetics should tend towards monophasic. Similarly, ΔA_{397} will reflect quinone arriving rapidly after the flash and will, therefore, titrate as $K_{Q_B}^{L}/(1 + K_2)$. This was shown previously for Q-0 [29].

The availability of quinone as a result of inter-micelle exchange is quite temperature dependent and is very variable from one detergent to another. We have found, for example, that Brij 58, a large, alkyl polyoxyethylene detergent, essentially seals the RC against further loss or gain of secondary quinone activity, at room temperature with Q-10. The smaller Brij 36, on the other hand, behaves quite similarly to Triton X-100, to which it is an alkyl equivalent.

The generally weaker binding of quinones to the Q_B site permitted us to determine the dissociation constants in lower detergent levels than those employed for Q_A reconstitution, and 0.1% LDAO was used routinely. Some comparisons were made with other detergent concentrations and types, and the effective parameter for hydrophobic quinones was found always to be the mole fraction in detergent, X_q^{det} (Fig. 3).

Results

Binding affinities for the Q_A site

Typical titrations of Q_A activity are shown in Fig. 4. The dissociation constants for the binding of various ubiquinones to the Q_A site are summarized in Table I, both in terms of bulk phase concentrations (K_{Q_A}) and on a mole fraction basis ($-\log X_{Q_A}^{det}$). It is apparent from these data that the binding affinities of the ubiquinones are not detectably sensitive to the length of the isoprene side-chain, providing it is at least two isoprene units long (Q-2). In 0.3% LDAO, the dissociation constants for all ubiquinones from Q-10 through Q-2 were $K_{Q_A} = 0.26 \pm 0.02$ μM, or $-\log X_{Q_A}^{det} = 4.71 \pm 0.05$. Even Q-1 bound with an affinity barely different from the longer chain forms ($K_{Q_A} = 0.48$ μM; $-\log X_{Q_A}^{det} = 4.4$). This seems to suggest a minimal influence of the isoprenyl side-chain in determining the binding properties of ubiquinones to the Q_A site.

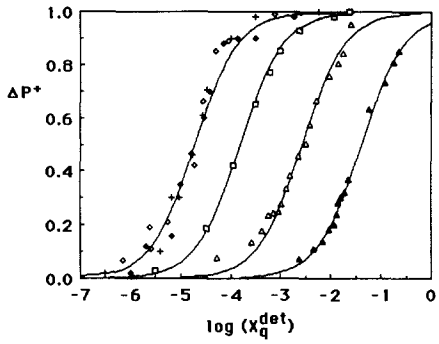

Fig. 4. Reconstitution of Q_A activity by various ubiquinones and analogues. Conditions: 10 M Tris (pH 8.0); ubiquinones – Q-10 (+), Q-9 (◆), Q-6 (◇) and decyl-Q-0 (□) – and plastoquinone A (△) in 0.3% LDAO; trimethylbenzoquinone (▲) in 0.1% LDAO. Lines are drawn for complete reconstitution with apparent binding affinities ($-\log X_{Q_A}^{det}$), from left to right, of 4.7, 3.8, 2.5 and 1.5.

TABLE I

Dissociation constants and van 't Hoff enthalpies and entropies of binding for ubiquinone species (Q-n) at the Q_A site in reaction centers [a]

Q-*n*	K_{Q_A} (μM)	$-\log X_{A_A}^{det}$ [b]	log P [c]	ΔG^0	ΔH^0 (kJ/mol) [d]	$-T\Delta S^0$
Q-10	0.19	4.8	≫ 5	−27.6	15.4	−42.9
Q-9	0.34	4.6	≫ 5	−26.1	14.1	−38.7
Q-8	0.29	4.7	≫ 5	−26.5	–	–
Q-7	0.20	4.8	≫ 5	−27.5	7.5	−35.2
Q-6	0.33	4.6	≫ 5	−26.3	−9.2	−17.3
Q-5	0.24	4.7	≫ 5	−27.0	−11.8	−15.2
Q-4	0.27	4.7	≫ 5	−26.7	−10.5	−16.4
Q-3	0.27	4.7	≫ 5	−26.7	–	–
Q-2	0.18	4.9	≫ 5	−27.7	−11.8	−15.8
Q-1	0.48	4.4	3.1	−25.3	−18.5	−6.9
		(4.5) [e]		(−25.9) [e]		
Q-0	40 *	(4.1)	0.9	(−23.4)		
methyl-Q-0	6.5 *	(4.3)	1.5	(−24.6)		
decyl-Q-0	2.1	3.8	> 5	−21.6		
	0.8 *	3.7		−21.3		

[a] Conditions: 10 mM Tris (pH 8.0)/0.3% LDAO, 298 K, except * determined in 0.1% LDAO.

[b] $X_{Q_A}^{det}$ is the mole fraction equivalent of K_{Q_A}, calculated as K_{Q_A}/[LDAO], with the detergent concentration in molar units: 0.3% = 13.1 mM, 0.1% = 4.36 mM.

[c] Coefficients for partition between octanol and water taken or estimated from data collected in Ref. 25; see text.

[d] The thermodynamic parameters are obtained from the binding data in mole fraction units.

[e] Values in parentheses are mole fraction equivalents of K_{Q_A}, calculated for the detergent phase alone by taking account of the partition coefficients, as described in the text.

TABLE II

Electron acceptor functions for various quinones reconstituted into 0Q reaction centers [a]

Quinone [b]	K_{Q_A} (μM)	$-\log X_{Q_A}^{det}$ [c]	log P [d]	k_{Q_A} (s^{-1})	$\Delta 2/\Delta 1$ [e]
Q-10	(0.03) [f]	4.7 *	$\gg 5$	9.0	0.88
Q-0	40	(4.1)	0.9	8.8	0.84
PQ-A	30/43 *	2.2/2.5 *	$\gg 5$	8.9	0.01
PQ-B	6	2.8	$\gg 5$	7.9	< 0.1
PQ-C	20	2.3	$\gg 5$	7.7	< 0.1
MK-8	(0.08) [f]	4.9 *	$\gg 5$	15.7	0.04
Phytyl-MK-0	0.4	4.1	$\gg 5$	14.1	0.12
MK-0	5.7	(3.8)	2.1	8.7	0.19
D-α-TQ	8.5	–	–	7.5	0.24
mBQ	2670	(2.7)	0.45	–	–
2,5-di-mBQ	1250	(2.4)	1.1	–	–
2,6-di-mBQ	770	(2.6)	1.1	–	–
Tri-mBQ	140	(2.8)	1.7	2.7	0.15
Tetra-mBQ (DQ)	0.7	(4.2)	2.7	1.7	0.09

[a] Conditions: 10 mM Tris (pH 8.0)/0.1% LDAO, 298 K, except * determined in 0.3% LDAO.

[b] Q, ubiquinone; PQ, plastoquinone; MK, menaquinone; TQ, tocopherolquinone; mBQ, methylbenzoquinone; DQ, duroquinone.

[c] Mole fraction equivalents of K_{Q_A} ($X_{Q_A}^{det} = K_{Q_A}/[LDAO]$, with the detergent concentration in molar units); values in parentheses are calculated for the detergent phase alone, taking account of the partition coefficients, as described in the text.

[d] Partition coefficients from water into cyclohexane (or octanol for Q-0, see text), are taken or estimated from data collected in Ref. 25.

[e] Ratio of cytochrome *c* oxidation after the second ($\Delta 2$) and first ($\Delta 1$) of two flashes given 50 ms apart, in the presence of excess quinone: 40 μM for Q-10, MK-8, and phytyl-MK-0, 2 mM for Q-0, 200 μM for PQ-A, B and C, 500 μM for D-α-TQ, and saturated solutions for tri- and tetramethylbenzoquinones.

[f] K_{Q_A} values for Q-10 and MK-8 are only approximate due to their very high affinities in 0.1% LDAO. The corresponding mole fraction values were determined in 0.3% LDAO.

The constancy of the affinity as the side-chain is shortened from 50 carbon atoms (Q-10) to 5 (Q-1) is in marked contrast to the effect of removal of the last isoprene unit. The affinity for Q-0, on a molar basis, is apparently much weaker than for Q-1 and, even in 0.1% LDAO, K_{Q_A} was 40 μM. Representation of the dissociation constant in mole fraction terms, by simply dividing by the detergent concentration, is misleading for Q-0 because it is sufficiently water-soluble as to be almost insensitive to detergent concentration, in the experimental range (0–1%). This will be developed further, below.

For 2,3-dimethoxy-5,6-dimethylbenzoquinone (methyl-Q-0), K_{Q_A} was 6.5 μM in 0.1% LDAO and was also not very sensitive to the detergent concentration. This is consistent with its significant water solubility (log P = 1.6, estimated in octanol). Decyl-Q-0, on the other hand, responded almost ideally to the detergent concentration, with $K_{Q_A} = 2.1$ μM in 0.3% LDAO and 0.8 μM in 0.1% LDAO ($-\log X_{Q_A}^{det} = 3.75$). It is noteworthy that the affinity for decyl-Q-0 is an order of magnitude weaker than that for Q-2, which has the same number of carbon atoms in the side-chain. Although the partition coefficients of these two ubiquinone derivatives may not be identical, the binding affinity is evidently not very sensitive to this parameter once the quinone is substantially partitioned into the detergent phase. Thus, a degree of structural specificity is indicated by this result.

Further structural specificities were revealed by the relative inability of plastoquinones (PQ, 2,3-dimethyl-5-isoprenylbenzoquinone) to reconstitute Q_A activity. Binding affinities for these and some closely related quinones are shown in Table II. Of the plastoquinones, PQ-A bound especially weakly ($K_{Q_A} \doteq 43$ μM in 0.3% LDAO, and 30 μM in 0.1% LDAO; $-\log X_{Q_A}^{det} =$ 2.5–2.2). The greatest affinity was displayed by PQ-B ($K_{Q_A} = 6$ μM in 0.1% LDAO; $-\log X_{Q_A}^{det} = 2.8$), a mixture of derivatives in which the first or second isoprene unit is hydroxylated and esterified to an aliphatic carboxylic acid of varying length. Plastoquinone C is the unesterified form. Considering the length of the isoprene side-chain in these naturally occurring plastoquinones ($n = 9$), these binding affinities further support the relative unimportance of this feature. Indeed, they are surprisingly weak and suggest a structural requirement for full substitution of the quinone ring.

A small selection of naphthoquinones was also assayed for Q_A-site binding, and revealed generally strong affinities, as previously reported by Gunner and Dutton [10,26]. Menaquinone-8 (MK-8, vitamin K-2, 2-methyl-3-octaisoprenyl-1,4-naphthoquinone) and phylloquinone (methyl-MK-0, vitamin K-1, 2-methyl-3-phytyl-1,4-naphthoquinone) both bound comparably

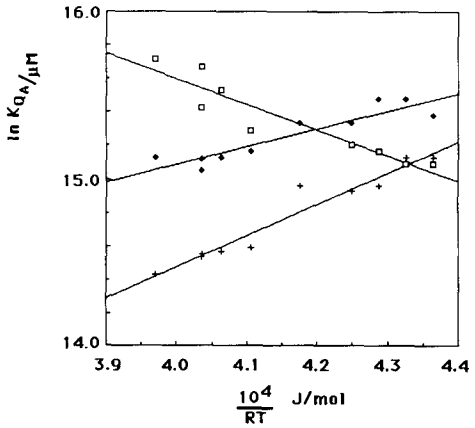

Fig. 5. Temperature dependence and thermodynamic parameters for Q_A reconstitution by prenyl ubiquinones. Van 't Hoff plot for Q-10 (□), Q-4 (◆) and Q-1 (+). Approx. 0.5 μM RCs, 0.3% LDAO, 10 mM Tris (pH 8.0). The derived thermodynamic parameters (ΔG^0, ΔH^0 and $-T\Delta S^0$) for these and other prenylogues are given in Table I.

with the prenyl ubiquinones. Menadione (MK-0, vitamin K-3, 2-methyl-1,4-naphthoquinone), which lacks the isoprene chain altogether, bound with an apparent affinity similar to that of methyl-Q-0 and more tightly than Q-0, the tail-less headgroup of the ubiquinone series.

Temperature dependence of binding to the Q_A site

Although the binding affinity at room temperature changed very little in the ubiquinone isoprenoid series, the temperature dependence of binding varied markedly with isoprene chain length. Fig. 5A shows the temperature dependence of K_{Q_A}, in 0.3% LDAO, for three ubiquinones, and it is clear that the long- and short-chain derivatives differ significantly in their responses. The derived data for all ubiquinone prenylogues are summarized in Table I. For the long-chain derivatives, the enthalpic contribution is actually unfavorable ($\Delta H^0 > 0$) and net binding is driven entirely by a large entropic term. However, the relative contributions of the enthalpic and entropic terms change as the side-chain is shortened. At $n = 6$, the enthalpy of binding changes sign and it becomes progressively more negative as further isoprene units are removed. Since the net free energy of binding remains constant throughout the ubiquinone series, this seems to represent a clear case of enthalpy/entropy compensation [33–35].

Binding affinities for the Q_B site

Table III shows values of K_{Q_B} and $-\log X_{Q_B}^{det}$ for all ubiquinones, determined predominantly by measuring ΔS, the amplitude of the slow phase of the recombination kinetics. The general trends are similar to those seen for Q_A reconstitution and there is no marked influence of the side chain length beyond one isoprene unit. The three assays described in Materials and Methods – the amplitude of the $Q_A^- Q_B \rightarrow Q_A Q_B^-$ electron transfer (e.g., ΔA_{397}), ΔS, and cytochrome turnover ($\Delta 2/\Delta 1$) – probe the functional binding of Q_B at progressively longer times after the flash. For Q-10, in LDAO, all three methods agreed well, with $-\log X_{Q_B}^{det} = 3.4 \pm 0.1$. However, for the shorter chain ubiquinones, even upto Q-6, the longer time assays showed stronger binding. We interpret this to indicate that these binding assays are variously affected by post-flash uptake of quinone, driven by the electron transfer equilibrium, so as to partially reflect the binding affinity for the semiquinone state (Eqn. 3) [18,29,31]. In LDAO, Q-10 is almost immobile on the time scale of all these assays and is adequately described by the pre-flash equilibrium, $K_{Q_B}^D$, in all cases. The shorter chain species are more mobile, however, and the ΔS and cytochrome turnover assays are displaced in the direction of $K_{Q_B}^L/(1 + K_2)$. For unified comparison of the various ubiquinone prenylogues, therefore, it may be better to take the shorter time assay (ΔA_{397}), indicative of $K_{Q_B}^D$. This shows a more marked drop in binding affinity for the shorter-chain quinones, Q-2 and Q-1.

The binding of Q-0 is also consistent with this trend. The assay for this species was different again, however,

TABLE III

Dissociation constants for the binding of ubiquinone species (Q-n) at the Q_B site in reaction centers [a]

Q-*n*	K_{Q_B} (μM) [b]	$-\log X_{Q_B}^{det}$ [c]
Q-10	1.7 ± 0.4 [d]	3.4 ± 0.1 [d]
Q-9	2	3.3
Q-7	3.5	3.1
Q-6	4	3.0
Q-5	4.5	3.0
Q-4	3	3.2
Q-3	3	3.2
Q-2	2.2 ± 1.4	3.3 ± 0.3
	9 [e]	2.7
Q-1	10	2.6 (2.9)
	70 [e]	1.9 (2.1)
Q-0	600 [f]	(2.8)
methyl-Q-0	135 [f]	(3.0)
decyl-Q-0	9	2.7 ± 0.5

[a] Conditions: 10 mM Tris (pH 8.0)/0.1% LDAO, 298 K.

[b] K_{Q_B} were determined by titration of ΔS, except as described in Notes d, e and f.

[c] $X_{Q_B}^{det}$ is the mole fraction equivalent of K_{Q_B}, calculated as K_{Q_B}/[LDAO], with the detergent concentration in molar units: 0.1% = 4.36 mM. Values in parentheses are calculated mole fraction data, for the detergent phase alone, taking account of the partition coefficients in octanol (see Table I), as described in the text.

[d] Values for Q-10 are the average of determinations using three assay methods: ΔS, ΔA_{397} and $\Delta 2/\Delta 1$ – see Methods.

[e] K_{Q_B} determined by titration of the amplitude of the millisecond phase of ΔA_{397}.

[f] K_{Q_B} determined by titration of k_{Q_B}, the rate of the slow recombination phase, yielding $k_{Q_B}^\circ$ by extrapolation to $[Q]^{-1} = 0$.

as it is substantially soluble in the aqueous phase, is rapidly mobile after the flash and can equilibrate fully to give further binding, driven by the electron transfer from Q_A^- to Q_B [29]. The dissociation constant was obtained from the quinone concentration dependence of the rate of the recombination reaction [29], yielding $K^L_{Q_B} = 360$–660 μM, at 298 K. The equivalence of $K^D_{Q_B}$ and $K^L_{Q_B}$ is uncertain. We have suggested that the redox state of Q_A/Q_A^- can affect the properties of Q_B and the Q_B binding site, and the influence that inhibitors of Q_B binding have on the redox midpoint potential (E_m) of Q_A is consistent with this [36]. However, the interpretation of this data is complex and it may be that only quinol binding is affected. Direct measurement of the binding of terburyn did not reveal an effect of the redox state of Q_A [23]. For present purposes, it is reasonable to compare $K^L_{Q_B}$, for Q-0, with $K^D_{Q_B}$ obtained for the other ubiquinones, and note the continued trend towards weaker binding as the isoprene chain is removed. Methyl-Q-0 behaved similarly to Q-0, with $K^L_{Q_B} = 135$ μM.

Temperature dependence of Q_B function

The effect of temperature on Q_B binding and properties was investigated with Q-0 as Q_B because the nature of the experimentally accessible parameters is well defined for this quinone and does not vary with temperature. In contrast, the mobility of the larger quinones increases substantially with temperature, so that the major influence on Q_B function changes from $K^D_{Q_B}$ to $K^L_{Q_B}$ (and K_2) as the temperature is raised (unpublished observations). Fig. 6 shows the temperature dependence of $K^L_{Q_B}$ and K_2 for Q-0, obtained from the kinetics of the recombination reaction as a function of quinone concentration. The data include one point at 17°C, from an earlier study done in 0.1% Triton X-100 [29], and the general agreement with the present work emphasizes the independence of Q-0 form the detergent

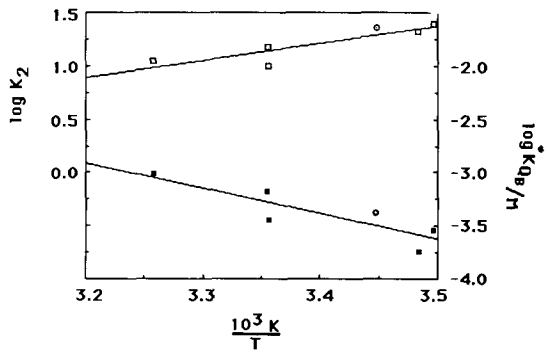

Fig. 6. Temperature dependence of Q_B activity by Q-0. K_2, the electron transfer equilibrium between $Q_A^-Q_B$ and $Q_AQ_B^-$ (□), and $K^L_{Q_B}$, the dissociation constant for quinone after the flash (■), were determined from the quinone (Q-0) concentration dependence of the rate of recombination (k_{Q_B}), at various temperatures. Conditions: approx. 1 μM RCs, 10 mM Tris (pH 8.0), 0.1% LDAO (except ○ and ●, taken from Ref. 29: 10 mM Tris (pH 8.2), 0.06% LDAO).

milieu. In spite of a substantial margin of error, the trend in the data is quite clear. The dissociation constant is strongly temperature-dependent, with a binding enthalpy ($\Delta H^\circ_{K_{QB}}$) of -36 ± 7 kJ/mol. At 298 K, the standard free energy of binding, $\Delta G^\circ_{K_{QB}}$, is -18.5 kJ/mol, yielding $-T\Delta S^\circ_{K_{QB}} \approx 27$ kJ/mol. The standard enthalpy for the electron transfer equilibrium (ΔH°_{K2}) is about -31 ± 6 kJ/mol. At 298 K, ΔG°_{K2} is -7.5 kJ/mol, so $-T\Delta S^\circ_{K2} \approx 23$ kJ/mol.

Electron transfer from Q_A^- to Q_B

At a fixed concentration of quinone (100 μM), the rate of electron transfer from Q_A^- to Q_B shows little dependence on the length of the ubiquinone side-chain, except for Q-1 ($t_{1/2} = 115 \pm 5$ μs for Q-10 through Q-2, and $t_{1/2} = 175$ μs for Q-1, in 0.1% LDAO; not shown). However, for Q-0, the rate of transfer was previously shown to be largely second-order, saturating at high concentrations as the binding site becomes fully occupied at the time of the flash [29]. In view of the relatively weak binding ($K^D_{Q_B}$) of Q-1, we consider it likely that the slower kinetics for this prenylogue arise, in part, from lack of saturation of the Q_B site, together with significant reequilibration of quinone after the flash, from within the same micelle *.

The one-electron equilibrium constant (K_2) between $Q_A^-Q_B$ and $Q_AQ_B^-$ is an important parameter for the continuous turnover of the acceptor quinone complex, as residence of the electron on Q_A will contribute to failures in the photochemical conversion (closed RCs). The efficacy of various ubiquinones in reconstituting Q_A to Q_B electron transfer in extracted RCs is shown in Fig. 7. K_2 was determined from the ratio of k_{Q_A} and the slow recombination rate constant determined at high quinone concentrations (ideally $k^\circ_{Q_B}$, as described in the Materials and Methods section). The value of K_2 falls off as the side chain is shortened below about six isoprene units. In view of the relative insensitivity of other parameters, such as binding affinity, to chain lengths in excess of three isoprene units, this is a little surprising, but it does correlate with the changing contributions of enthalpic and entropic terms of the binding free energy for Q_A (Table I). The possibility that the value of k_{Q_B} determined was not maximal, i.e., yielding K_2^{app} rather than K_2, was investigated by repeating the measurements at very low detergent (0.001% LDAO) or at low temperature (8–13°C), when quinone mobility between micelles is negligible. These measurements resulted in small increases in the relative values of K_2 for

* The cmc for LDAO is approx. 0.048% (2.1 mM) and the aggregation number is 75. Thus, in 0.1% LDAO (4.4 mM) the concentration of micelles is roughly 30 μM and, with 100 μM quinone, almost every micelle should have at least one Q-1 (Poisson distribution).

Q-1 and Q-2, but did not alter the general trend in the data.

In 11 different preparations of each type (0Q- and 1Q-RCs, in 0.1% LDAO), full reconstitution with Q-10 in 0Q RCs gave a slow recombination time that was 8% faster than for 1Q RCs (799 ± 9 vs. 862 ± 17 ms). The difference was statistically significant, but the corresponding change in K_2 is barely detectable in most functional assays. Apart from this small systematic difference, the effect of ubiquinone substitution on K_2 was essentially the same for 0Q- (Q-*n* as Q_A and Q_B) and 1Q-RCs (Q-10 as Q_A in all cases), indicating that the effect of chain length is exerted through the redox potential of the Q_B/Q_B^- couple alone.

In contrast to the short-chain isoprenyl ubiquinones, Fig. 7 shows Q-0 and methyl-Q-0 to elicit substantial increases in K_2, in 1Q-RCs. This apparently paradoxical behavior is fully consistent with the intrinsic redox properties of these species, which have higher in vitro midpoint potentials than any of the isoprenyl forms [7]. This is discussed further, below.

Although reconstitution of Q_A is observed with a wide variety of quinone species, it has generally been held that Q_B function is much more specific [44]. This appears to be true for reconstitution of 0Q-RCs, where the non-native quinone must function as both Q_A and Q_B (Table II). In assays of turnover of the acceptor quinones by the ability to oxidize cytochrome on the second flash of a pair given 50 ms apart ($\Delta 2/\Delta 1$), Q-10 and Q-0 reconstituted into 0Q-RCs both gave more than 80% turnover on the second flash. This level of activity is typical of fully extracted, reconstituted reaction centers (0Q-RCs). When reconstituted with

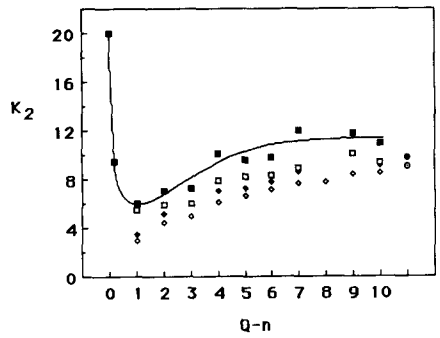

Fig. 7. Variation of the electron transfer equilibrium between $Q_A^- Q_B$ and $Q_A Q_B^-$ (K_2) with isoprene chain length. K_2 was determined from the ratio of the fast and slow recombination rates for various prenyl ubiquinones (Q-*n*, where *n* indicates the number of isoprene units in the side chain). The fast recombination rate was determined in the absence of added ubiquinone (1Q-RCs) or in the presence of substoichiometric amountQ-RCs); the slow rate was determined in the presence of 100 μM prenyl ubiquinone. Conditions: all measurements in 10 mM Tris (pH 8.0); ◇, 0Q-RCs in 0.1% LDAO, 25 °C; ◆, 1Q-RCs in 0.1% LDAO, 25 °C; □, 1Q-RCs in 0.001% LDAO, 25 °C; ■, 1Q-RCs in 0.1% LDAO, 13 °C. Averages of 11 separate preparations and extractions, reconstituted with Q-10 (in 0.1% LDAO, 25 °C) are shown for 0Q-RCs (⊙) and 1Q-RCs (●).

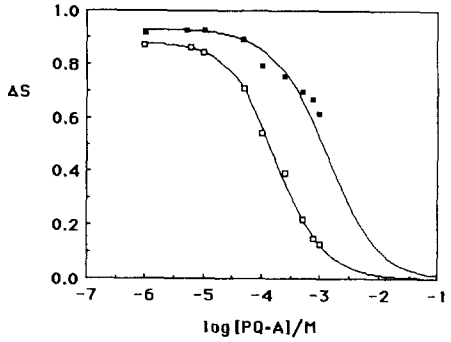

Fig. 8. Competitive inhibition by plastoquinone at the Q_B site. The amplitude of the slow phase of recombination, with Q-10 as Q_B, is shown as a function of PQ-A concentration. 0.5 μM RCs in 10 mM Tris (pH 8.0), 0.1% LDAO, plus 6 μM (□) or 40 μM (■) Q-10. Curves are drawn according to: $\Delta S_{max} = 0.98$, K_{Q_B}(Q-10) = 0.8 μM ($-\log X_{Q_B}^{det} = 3.7$), K_{QB}(PQ-A) = 30 μM ($-\log X_{Q_B}^{det} = 2.2$).

quinones other than ubiquinones, the second flash activity was small in all cases, but especially for menaquinone-8 and the plastoquinones, all of which should at least partition favorably into the detergent phase. On the other hand, we have previously shown [37] that menaquinone-8 as Q_A can readily transfer electrons to Q-10 as Q_B, with an enhanced equilibrium constant (K_2) consistent with the expected lower redox potential of menaquinone [7]. This was not tested for the plastoquinones because their weak binding as Q_A (Table II) renders then susceptible to displacement by any ubiquinone.

The failure of the plastoquinones to reconstitute the two-electron gate in bacterial RCs, is particularly surprising in view of the fact that PQ-A fulfills both Q_A and Q_B roles in RCs of Photosystem II in higher plants, algae and cyanobacteria. They also failed to function as Q_B in 1Q-RCs, with Q-10 as Q_A. Since the plastoquinones bind weakly as Q_A, we considered that their binding as Q_B might be so weak as to be essentially absent. This was tested by titration of fully active RCs (with Q-10 as Q_A and Q_B) with PQ-A, to see if the plastoquinone was a competitive inhibitor of the Q_B activity of Q-10. Fig. 8 shows that, indeed, Q_B activity was inhibited by PQ-A, with an inhibitor dissociation constant of 30 μM in 0.1% LDAO ($-\log X_{Q_B}^{det} = 2.2$), compared with 0.8 μM for Q-10 ($-\log X_{Q_B}^{det} = 3.7$). It is noteworthy that the affinity of PQ-A for the Q_B site is very similar to that observed for binding to the Q_A site (Table II). A similar inhibition of Q_B function was also seen for duroquinone (not shown).

Discussion

The work described here provides a view of the binding and functional properties of the acceptor quinones of bacterial reaction centers, focusing on the relative roles of the headgroup and isoprene side-chain as determinants of function.

Establishing a comparative basis for Q_A binding

A quantitative description of the relative importance of headgroup features for binding of natural isoprene-substituted quinones, is confounded by the significant, but differential, water solubilities of the smaller quinones. In the case of the methylbenzoquinones, including plastoquinone, duroquinone provides a link between the water-soluble species and the very hydrophobic, long-chain forms. For the di- and trimethyl benzoquinones, which are quite water-soluble (> 1 mM), with relatively small partition coefficients (log $P \leq 2$), the measured (net) binding affinities in 0.1% LDAO closely reflect the affinities based on the aqueous concentrations. These may be compared directly with the low detergent limit for duroquinone ($K_{Q_A} = 0.5$ μM) (Fig. 1). The plastoquinones, on the other hand, are solubilized exclusively in the detergent phase and their binding affinities ($-\log X_{Q_A}^{det} = 2.2$ to 2.8) must be compared with the detergent phase value for duroquinone, which may be obtained by extrapolation of the data of Fig. 1 to high detergent, or by calculation using a partition coefficient, log P, of 2.7. Both approaches yield $-\log X_{Q_A}^{det} \approx 4.2$ *. The binding affinities for 2,5- and 2,6-dimethyl- and trimethylbenzoquinone can also be estimated for the detergent phase, using partition coefficients (log P) of 1.1 and 1.7, for the di- and trimethylbenzoquinones, respectively [25]. The calculated values are $-\log X_{Q_A}^{det} = 2.4$, 2.6 and 2.8, very similar to the range of values for the plastoquinones. The significantly higher value for duroquinone, compared to trimethylbenzoquinone and the plastoquinones, dramatically reveals the stronger binding of the fully ring-substituted quinone, and the relative ineffectiveness of a large, hydrophobic tail structure. This indicates that a major contribution comes from contact interactions, such as van der Waals forces, in the headgroup region, as clearly shown by the work of Gunner and Dutton [9,10,26]. The trend in the di-, tri- and tetramethylbenzoquinones is clearly towards tighter binding as the degree of ring substitution increases, although the values for the dimethylbenzoquinones are, perhaps, not as small as expected. Similarly, the detergent phase binding affinity for methylbenzoquinone ($-\log X_{Q_A}^{det} = 2.6$, log $P = 0.6$) is unexpectedly high. These discrepancies may arise from the relatively larger errors in small values for the partition coefficients of these compounds.

D-α-Tocopherolquinone (2,3,5-trimethyl-6-(3′-hydroxy)tetraisoprenylbenzoquinone), a fully substituted benzoquinone, appears to bind quite weakly (Table II), but it is possible that the hydroxylated nature of its rather short and saturated side-chain gives it a significantly smaller partition coefficient than the equivalent isoprenyl quinones. This is certainly consistent with its very low chromatographic mobility in apolar solvents [15].

Examination of dimethoxybenzoquinones – Q-0, methyl-Q-0 and the ubiquinone series – also indicates only a weak contribution of the side-chain to the net binding strength. Q-0 and methyl-Q-0 are much more water-soluble than their methyl counterparts, tri- and tetramethylbenzoquinone, and neither Q-0 nor methyl-Q-0 exhibits sufficient detergent dependence to obtain a $-\log X_{Q_A}^{det}$ value, directly, for comparison with very hydrophobic quinones. The best we can do with the available data is assume proper equilibrium between the aqueous and detergent phases for these smaller ubiquinones, and estimate detergent phase binding affinities to compare with the measured affinities of the isoprene-substituted ubiquinones. With log P values of about 0.9 and 1.5 for Q-0 and methyl-Q-0, respectively (Ref. 25, and see discussion above), we can calculate $-\log X_{Q_A}^{det}$ values of 4.1 and 4.3, compared to 4.5 for Q-1 (log $P = 3.1$) and 4.7 for the higher prenylogues (Q-10 through Q-2, log $P > 5$). The small partition coefficients for Q-0 and methyl-Q-0 render these estimates rather crude, but the similarity between all the values emphasizes the lack of a strong influence of the tail when binding equilibrium is established between the protein and a hydrophobic phase. The affinity for Q-0 may appear unexpectedly high compared, for example, to trimethylbenzoquinone, but it presumably reflects the greater size. This is supported by the similar affinity (on a mole fraction basis, see Table II) exhibited by MK-0 (2-methylnaphthoquinone: $-\log X_{Q_A}^{det} = 3.8$, log $P = 2.1$), a molecule of very similar size to Q-0. It also supports a lack of any great chemical specificity for the methoxy groups, a conclusion that has been forcefully made by Gunner and Dutton [10] on the basis of extensive comparisons with many small quinones.

An alternative basis for a unified comparison of the ubiquinones is to estimate a low detergent (i.e., aqueous phase) limit for Q-1 binding, since this quinone is sufficiently amphipathic that both phases can be taken as in equilibrium *. For Q-1, with log $P \approx 3.1$, we calculate from $-\log X_{Q_A}^{det} = 4.4$ (Table I) that $K_{Q_A} \approx 0.1$ μM in the water phase. The values for all these parame-

* From an apparent dissociation constant, K_{Q_A} (μM), measured in x% detergent (molecular weight, MW_{det}), the binding affinity in terms of the detergent phase can be determined as follows:

$$X_{Q_A}^{det} = \frac{K_{Q_A} \cdot MW_{det}}{(x\%) + 100/P} \cdot 10^{-7}$$

where P is the partition coefficient of the quinone between the water and detergent phases – here approximated by partition into cyclohexane or octanol. This expression makes the approximation that the volume of the aqueous phase is equal to the total volume.

* See footnote, p. 168 left-hand column.

ters are quite similar to those described above for duroquinone.

Headgroup and tail contributions to quinone binding and function

Our analysis in terms of equilibrium from the detergent phase reveals novel aspects of the binding specificity and specifically deemphasizes the contributions of the tail. For both Q_A and Q_B, it seems that only the first two (Q_A) or three (Q_B) isoprene units make net contributions to the binding affinity. This is also sufficient to ensure that the quinone is entirely ($\gg 99\%$) partitioned into the detergent phase, and we suppose that the function of the tail, in vivo, is at least partly along similar lines. The much longer tails encountered in vivo may arise for reasons of stability – the short chain ubiquinones, Q-4 and smaller, are notably more susceptible to oxidative cyclization of the first isoprene unit to the headgroup ring – or to localize the quinones within the lipid bilayer, for example in the mid-plane [38].

However, the side-chain may not be irrelevant to function, and the lack of a major contribution of the tail to the overall energetics of binding does not preclude significant interaction in this region. The detergent-phase binding affinity of decyl-Q-0 ($-\log X_{Q_A}^{det} = 3.7$) is about 10-times weaker than for Q-2, suggesting that a hydrophobic tail can be a liability if it is not of the right structural form. This provides some support for specific side-chain interactions, especially in the first two or three isoprene subunits. Indeed, studies on short alkyl chain-substituted ubiquinones have shown surprising details of specificity in the first few carbon-carbon bonds [39]. Furthermore, the progressive change in thermodynamic contributions to the binding free energy of Q_A, as the tail is shortened (Table I) indicates compensating shifts in the nature of the binding, with a significant jump in behavior between Q-7 and Q-6 *. We have suggested that the enthalpic contribution, which is dominant in the short-chain ubiquinones, is indicative of headgroup interactions, while the entropic term reflects binding of the hydrophobic tail [35]. Since the net affinity is almost unchanged throughout the ubiquinone series, the increased hydrophobic interactions of the longer tails would seem to be at the expense of interactions in the headgroup region. This may suggest that the tail tends to pull the head away, which could cause energetic or structural perturbations of Q_A function. The latter is supported by the fact that the $P^+Q_A^-$ recombination reaction, at low temperatures, is distinctly slower for Q-0 (10 s^{-1} at 110 K) than for Q-10 (35 s^{-1}) (not shown). At room temperature, however, we found all ubiquinones (Q-10–Q-0) to exhibit similar recombination rates (8–9.5 s^{-1}). Q-0 is unusual in not exhibiting any significant acceleration of the recombination rate at low temperatures. Acceleration is typical for RCs from *Rb. sphaeroides* with all but the most low-potential quinones as Q_A [9]. Possibly the small size of Q-0 may allow some structural rearrangements as the temperature is lowered, thereby masking the expected acceleration with a secondary effect.

An antagonistic effect of the headgroup and tail is also suggested in Q_B function by the observation that the presence of 2 mM farnesol, as an analogue of a short isoprenyl chain, caused a 6-fold decrease in the apparent binding affinity of Q-0, as Q_B, and a 1.7-fold decrease for methyl-Q-0 (not shown). In view of the hydrophilic nature of these quinones and the significant level of detergent already present (4.3 mM), it is unlikely that this effect is simply due to dilution of the quinone in the additional hydrophobic phase.

Small changes in the energetics of Q_A^- are likely to have little effect on the primary kinetic behavior of the RC, since the rates of I^- to Q_A electron transfer and the direct $P^+Q_A^-$ recombination are almost insensitive to the E_m of Q_A/Q_A^- in the potential range provided by the quinones used in this study [9,40]. However, the activated recombination route, via P^+I^-, may detect some energetic shifts in Q_A [22,40,41] and the direct, tunnelling route is likely to be sensitive to structural perturbations [9,42]. Of the various benzoquinones tested, all the ubiquinones and plastoquinones gave similar recombination rates at room temperature ($k_{QA} \approx 8$–$9\ s^{-1}$), but duroquinone gave a significantly slower rate (1.7 s^{-1}), as reported previously [21]. This cannot be a simple reflection of intrinsic redox energetics as the in vitro half-wave potential of the duroquinone Q/Q^- redox couple ($E_{1/2}$), in dimethylformamide (DMF), is about -405 mV, which is more negative than the ubiquinones ($E_{1/2} \approx -365$ mV) [7]. However, the extensive studies of Gunner and Dutton suggest that the in situ potential of duroquinone is unexpectedly higher

* For the very hydrophobic, long chain quinones the partition coefficients are so large that binding equilibrium from the water phase cannot be assumed on laboratory time scales. For Q-5, for example, log $P \approx 13$ [25] and for a net concentration of 100 μM quinone in 0.1% LDAO the actual concentration in the water phase will be no greater than 10^{-14} M. If equilibration between the RC and aqueous quinone is taken to occur via collisional encounters at the diffusion limit ($k \approx 10^9\ M^{-1} \cdot s^{-1}$) the on rate will be of the order of $10^{-5}\ s^{-1}$. The necessary time for equilibration quickly becomes astronomical for even longer chain prenylogues, for which log P increases by approximately 3 – a factor of 1000 in P – per isoprene unit [25].

* Proper assessment of enthalpic vs. entropic behavior would require analysis in terms of the detergent phase binding affinity, but the necessary temperature dependences of the partition coefficients and detergent micelle properties are not known in detail. However, available data on partition coefficients for small molecules between water and organic phases indicate only weak temperature dependences [24].

than that of ubiquinone [9,10,22].

The naphthoquinone isoprenoid derivatives, menaquinone-8 (MK-8) [37,41] and phylloquinone (phytyl-MK-0) gave significantly faster rates than the ubiquinones, while the rate for menadione (MK-0) was similar. These differences could possibly be of energetic origin. $E_{1/2}$ for both MK-8 and phytyl-MK-0 is −465 mV, but it is only −405 mV for MK-0 [7]. If the relatively lower potentials of MK-8 and phytyl-MK-0 are maintained in situ, they may be sufficiently negative to slightly enhance the thermal accessibility of the activated recombination route via P^+I^- [22,40,41]. This gains some support from the fact that, at low temperature, the recombination rate with MK-8 as Q_A becomes indistinguishable from that with Q-10 [9,41].

It should be noted that entropic contributions to binding, associated with hydrophobic interactions of the tail, are likely to be less significant in vivo, where the binding equilibrium is established between the protein site and the extensive hydrophobic solvent phase of the membrane. If this is so, then the Q_A headgroup interactions will be relatively more influential in vivo, even for the native, long-chain ubiquinones (Q-10, in *Rb. sphaeroides*). This may be a contributing factor to the observation that the $P^+Q_A^-$ recombination rate in chromatophores is faster than in isolated RCs ($t_{1/2}$ = 45 vs. 80 ms [43]).

Q_B binding and function

A very similar picture emerges for Q_B binding when the detergent phase is considered. For Q-0, methyl-Q-0, Q-1 and Q-2, taking the relevant partition coefficients into account, as above, $-\log X_{Q_B}^{det}$ is estimated to be 2.1–3.3. The variation is not obviously systematic with side-chain length – the range of values for Q-1 being 2.1 (from ΔA_{397}) to 2.9 (from ΔS) – and it is as likely to arise from inadequacies in the estimations as from a real structural source. Our values for Q-1 agree well with the data of Diner and co-workers [23], which yield $-\log X_{Q_B}^{det} = 2.8$ in 1.0% LDAO, and 2.2 in 0.025% LDAO, determined from the slow phase of the recombination kinetics. Thus, the binding affinities of these smaller ubiquinones are no more than an order of magnitude less than those measured here for the most hydrophobic, long-chain ubiquinones, e.g., for Q-10, $-\log X_{Q_B}^{det} = 3.4 \pm 0.1$; similarly, from Ref. 23, $-\log X_{Q_B}^{det} =$ 3.55 for Q-10, and 3.5 for Q-9. These comparisons imply, again, only a minor role for the side-chain in determining the overall affinity of the Q_B site for the ubiquinone structure.

The temperature-dependence of Q-0 activity as Q_B shows the binding to be enthalpically driven and substantially opposed by entropic contributions. This is consistent with the trend seen for binding of short-chain ubiquinones to the Q_A site. The diverse thermal properties of the two contributing processes of binding and electron transfer can lead to inscrutable behavior of the observed electron transfer equilibrium when Q_B binding is not saturated at all temperatures. With Q-10 as Q_B, at apparently saturating concentrations of quinone in 0.1% LDAO, we have measured ΔH_{K_2} to be −8.5 kJ/mol (not shown). Other reports in the literature indicate a rather large spread of values, viz., −22 kJ/mol in 0.025% LDAO [28], and −14.5 kJ/mol in 0.1% LDAO [44]. We have not been able to separate unambiguously the binding and electron transfer contributions for Q-10 because of changes in mobility of the quinone over a significant range of temperature, as described above. However, the range of reported values for ΔH_{K_2} could be consistent with a 'positive' binding enthalpy ($\Delta H_{K_{QB}}$) for Q-10 as Q_B, as observed for Q_A (Fig. 5 and Table I). The two smaller values for ΔH_{K_2} might then indicate some compensating effects of binding (positive $\Delta H_{K_{QB}}$) and electron transfer (negative ΔH_{K_2}), and it is noteworthy that they were obtained in higher detergent than the largest value, which is also the most similar to our value of ΔH_{K_2} for Q-0 as Q_B (−31 kJ/mol). Our analysis of Q-0 activity properly separates the parameters of binding and electron transfer for this analogue.

Reconstitution of Q_A and Q_B function

Of all the quinone species tested, only the ubiquinones were able to properly reconstitute both Q_A and Q_B function. However, it would be misleading to conclude that Q_B function was more specific or the Q_B binding site more discriminating than the Q_A site. The average affinity of the Q_B site is only 10–20-times weaker than that of the Q_A site. This is not an overwhelming distinction and is consistent with the general observation that partially extracted RCs exhibit some Q_B activity even when the Q_A site is not fully occupied. In the case of the plastoquinones, the binding affinity for PQ-A at the Q_B site was found to be very similar to that at the Q_A site, and quite sufficient to support substantial Q_B activity. Thus, the failure of the plastoquinones to exhibit Q_B function must lie elsewhere, probably with their in situ redox potential. This also provides a likely source of explanation for the peculiar abilities of the ubiquinones, which are uniquely flexible in their redox properties as has been well documented by studies on the polarographic halfwave potentials ($E_{1/2}$) of many quinones in DMF [7].

The methoxy groups characteristic of ubiquinones exhibit both the electron withdrawing properties of the oxygen, via the inductive effect, and electron donating properties, via the mesomeric effect [7,11,24]. The latter arises from delocalization of the unpaired *p*-orbital electrons of the oxygen over the enone and aromatic nucleus of the quinone/quinol structures. Effective delocalization requires alignment of the methoxy group in the plane of the ring. From the data of Prince at al. [7], it is evident that a single methoxy group is significantly

electron donating, as expected, resulting in a lower $E_{1/2}$ for the Q/Q^- couple of methoxy-1,4-benzoquinone (-265 mV vs. NHE) than for the unsubstituted species ($E_{1/2} = -157$ mV). Two methoxy groups placed on opposite sides of the quinone ring are essentially additive ($E_{1/2} = -426$ mV for 2,5-dimethoxy and -384 mV for 2,6-dimethoxy), but when positioned in the vicinal configuration they have less effect than one methoxy ($E_{1/2} = -214$ mV for 2,3-dimethoxy). Evidently the presence of the second disrupts the effect of the first. Molecular models show that the methoxy groups cannot both lie in the ring plane, due to steric hindrance with each other and with the carbonyl oxygens. This is confirmed by X-ray studies on crystals of Q-0 which show one methoxy in-plane and one almost at right angles to it [45]. Thus, the second methoxy group can only be electron-withdrawing. The energetic effects of this interaction have been qualitatively described to show a continuous variation of the redox potential as the methoxy groups are twisted [7,11], and this has been quantitatively simulated by molecular orbital calculations (Robinson, H.H. and Kahn, S., personal communication). A related effect on the partition coefficients of methoxy-substituted ring systems is also known [25].

With this in mind, it is easy to see how the ubiquinones could be uniquely suited to simultaneously filling the roles of Q_A and Q_B. The failure of PQ-A to function as Q_B with Q-10 as Q_A could be understood in terms of their respective in vitro $E_{1/2}$ values (-375 mV for PQ-A and -358 mV for Q-10 [7]), but the failure of PQ-A to function as both Q_A and Q_B clearly implies that the 'solvent-like' nature of the two binding domains is not sufficient to produce the redox potential difference needed to effect electron transfer from Q_A^- to Q_B. This is particularly striking, because from the X-ray structure it is apparent that Q_B is approx. 0.2 nm closer to the iron atom (1 net positive charge) than Q_A [5,46], which should make Q_B more electropositive than Q_A. Furthermore, studies on the pH dependence of the $Q_A^-Q_B \leftrightarrow Q_AQ_B^-$ electron transfer in native RCs show that the electron transfer equilibrium is not favorable unless H^+ ion binding occurs. This suggests that the inherent solvent properties of the Q_B pocket render the Q/Q^- couple more reducing, perhaps because of its more polar [46], and possibly more hydrated, nature.

In contrast to most quinones, the redox potential of ubiquinones can be further tuned by adjustments of the methoxy group orientations in the binding sites. It is not easy to assess the precise disposition of the methoxy substituents for Q_A and Q_B in RCs from *Rb. sphaeroides* from the published crystallographic data [5,46,47], but it is clear that they are very different. This fine-tuning option is not available to any of the other quinones tested, and we suggest that it is this which limits the function of, e.g., the plastoquinones in bacterial reaction centers. This raises the question of how PQ-A functions in Photosystem II, where it fills both Q_A and Q_B roles. Presumably the solvent-like environments of the two binding sites in Photosystem II are suffiicently different as to imprint the necessary redox potential span and it will be of interest to compare the bacterial and plant structures on this basis.

Acknowledgements

This work was supported by grants from the National Science Foundation (PCM 83-16487 and DBM 86-17144). J.C.M. and R.R.S. were supported, in part, by Public Health Service Traineeships from the National Institutes of Health.

References

1 Wraight, C.A. (1982) in Function of Quinones in Energy Conserving Systems (Trumpower, B.L., ed.), pp. 181–197, Academic Press, New York.
2 Crofts, A.R. and Wraight, C.A. (1983) Biochim. Biophys. Acta 726, 149–185.
3 Deisenhofer, J., Epp, O., Miki, K., Huber, R. and Michel, H. (1985) Nature 318, 618–624.
4 Michel, H., Epp, O. and Deisenhofer, J. (1986) EMBO J. 5, 2445–2451.
5 Allen, J.P., Feher, G., Yeates, T.O., Komiya, H. and Rees, D.C. (1987) Proc. Natl. Acad. Sci. USA 84, 5730–5734.
6 Allen, J.P., Feher, G., Yeates, T.O., Komiya, H. and Rees, D.C. (1987) Proc. Natl. Acad. Sci. USA 84, 6162–6166.
7 Prince, R.C., Dutton, P.L. and Bruce, J.M. (1983) FEBS Lett. 160, 272–276.
8 Prince, R.C., Lloyd-Williams, P., Bruce, J.M. and Dutton, P.L. (1986) Methods Enzymol. 125, 109–119.
9 Gunner, M., Robertson, D.E. and Dutton, P.L. (1986) J. Phys. Chem. 90, 3783–3793.
10 Gunner, M.R. and Dutton, P.L. (1989) J. Am. Chem. Soc. 111, 3400–3412.
11 Prince, R.C., Halbert, T.R. and Upton, T.H. (1988) in Advances in Membrane Biochemistry and Bioenergetics (Kim, C.H., Tedeschi, H., Diwan, J.J. and Salerno, J.C., eds.), pp. 469–478, Plenum Press.
12 Maróti, P., Levine, L.M.A., Holten, D. and Pearlstein, R.M. (1985) Biochim. Biophys. Acta 810, 132–139.
13 Okamura, M.Y., Isaacson, R.A. and Feher, G. (1975) Proc. Natl. Acad. Sci. USA 72, 3491–3495.
14 Dunphy, P.J. and Brody, A.F. (1971) Methods Enzymol. 18 C, 407–461.
15 Barr, R. and Crane, F.L. (1971) Methods Enzymol. 23, 372–408.
16 Takamiya, K. and Takamiya, A. (1969) Plant Cell Physiol. 10, 363–373.
17 Kröger, A. and Dadak, V. (1969) Eur. J. Biochem. 11, 328–340.
18 Stein, R.R. (1985) Ph.D. Thesis, University of Illinois, Urbana-Champaign.
19 Wraight, C.A. and Clayton, R.K. (1973) Biochim. Biophys. Acta 333, 246–260.
20 Kirmaier, C. and Holten, D. (1987) Photosynth. Res. 13, 225–260.
21 Pocinki, A.G. and Blankenship, R.E. (1982) FEBS Lett. 147, 115–119.
22 Woodbury, N.W., Parson, W.W., Gunner, M.R., Prince, R.C. and Dutton, P.L. (1986) Biochim. Biophys. Acta 851, 6–22.
23 Diner, B.A., Schenck, C.C. and De Vitry, C. (1984) Biochim. Biophys. Acta 766, 9–20.

24 Hansch, C. and Leo, A.J. (1979) Substituent Constants for Correlation Analysis in Chemistry and Biology, Wiley, New York.
25 Braun, B.S., Benbow, U., Lloyd-Williams, P., Bruce, J.M. and Dutton, P.L. (1986) Methods Enzymol. 125, 119–129.
26 Gunner, M.R., Prince, R.C. and Dutton, P.L. (1981) Biophys. J. 33, 171a.
27 Wraight, C.A. (1979) Biochim. Biophys. Acta 548, 309–327.
28 Kleinfeld, D., Okamura, M.Y. and Feher, G. (1984) Biochim. Biophys. Acta 766, 126–140.
29 Wraight, C.A. and Stein, R.R. (1983) in The Oxygen Evolving System of Photosynthesis (Y. Inoue et al., eds.), pp. 383–392, Academic Press, New York.
30 Crofts, A.R. and Wraight, C.A. (1983) Biochim. Biophys. Acta 726, 149–185.
31 McComb, J.C. (1987) Ph.D. Thesis, U. Illinois, Urbana-Champaign.
32 Wraight, C.A. and Stein, R.R. (1980) FEBS Lett. 113, 73–77.
33 Lumry, R.P. and Rajender, S. (1970) Biopolymers 9, 1125–1127.
34 Eftink, M.R., Anusiem, A.C. and Biltonen, R.L. (1983) Biochemistry 22, 3881–3896.
35 Wraight, C.A., Stein, R.R., Shopes, R.J. and McComb, J.C. (1984) in Advances in Photosynthesis Research (Sybesma, C., ed.), Vol. 1, pp. 629–636, Martinus Nijhoff/Dr. W. Junk, The Hague.
36 Wraight, C.A. (1981) Isr. J. Chem. 21, 348–354.
37 Shopes, R.J. and Wraight, C.A. (1985) Biochim. Biophys. Acta 806, 346–356.
38 Millner, P.A. and Barber, J. (1984) FEBS Lett. 169, 1–6.
39 Warncke, K., Gunner, M.R., Braun, B.S., Yu, C.-A. and Dutton, P.L. (1987) Biophys. J. 51, 124a.
40 Gunner, M.R., Liang, Y., Nagus, D.K., Hochstrasse, R. and Dutton, P.L. (1982) Biophys. J. 33, 226a.
41 Shopes, R.J. and Wraight, C.A. (1986) Biochim. Biophys. Acta 893, 409–425.
42 Feher, G., Okamura, M.Y. and Kleinfeld, D. (1987) in Protein structure: Molecular and Electronic Reactivity (Austin, R. et al., eds.), pp. 399–421, Springer-Verlag, New York.
43 Stein, R.R., Castellvi, A.L., Bogacz, J.P. and Wraight, C.A. (1984) J. Cell. Biochem. 24, 243–259.
44 Mancino, L.J., Dean, D.P. and Blankenship, R.E. (1984) Biochim. Biophys. Acta 764, 46–54.
45 Silverman, J., Stam-Thole, I. and Stam, C.H. (1971) Acta Cryst. B27, 1846–1851.
46 Allen, J.P., Feher, G., Yeates, T.O., Komiya, H. and Rees, D.C. (1988) Proc. Natl. Acad. Sci. USA 88, 8487–8491.
47 Chang, C.-H., Tiede, D., Tang, J., Smith, U., Norris, J. and Schiffer, M. (1986) FEBS Lett. 205, 82–86.